

Sound attenuation in low temperature amorphous solids is primarily determined by non-affine displacements

Grzegorz Szamel¹ and Elijah Flenner¹

¹*Department of Chemistry, Colorado State University, Fort Collins, Colorado 80523, USA*

(Dated: August 2, 2021)

Sound attenuation in low temperature amorphous solids originates from their disordered structure. However, its detailed mechanism is still being debated. Here we analyze sound attenuation starting directly from the microscopic equations of motion. We derive an exact expression for the zero-temperature sound damping coefficient and verify that it agrees with results of earlier sound attenuation simulations. The small wavevector analysis of this expression shows that sound attenuation is primarily determined by the non-affine displacements' contribution to the wave propagation coefficient coming from the frequency shell of the sound wave.

Introduction.— In classical crystalline solids sound attenuation originates from thermal motion of the particles. Its dependence on the sound wave's wavevector follows predictions of the solid's hydrodynamics [1, 2]; the sound attenuation scales as k^2 with the wavevector. It vanishes at zero temperature, where the sound waves propagate indefinitely.

The physics of sound attenuation in amorphous solids is drastically different. At low temperatures, when thermal effects can be neglected, sound is attenuated due to the inherent disorder of these solids. The attenuation has a complicated dependence on the wavevector [3], but small wavevector k^4 scaling of the attenuation has long been conjectured on an experimental basis [4, 5]. It was interpreted as the result of the Rayleigh scattering of sound waves from the solids' inhomogeneities. Recent computer simulations verified that in classical three-dimensional (3D) zero-temperature amorphous solids at the smallest wavevectors attenuation scales as k^4 [6–8], although a logarithmic correction to this quartic scaling was also claimed [9].

The specific physical mechanism of sound attenuation in low temperature amorphous solids is still debated. The Rayleigh scattering scaling was obtained [4] using an “isotopic scattering” [5] model in which every atom of the glass is an independent source of scattering. Several recent experimental and simulational results were analyzed within the framework of the fluctuating elasticity theory [10–12], which posits that an amorphous solid can be represented as a continuous medium with spatially varying elastic constants. The inhomogeneity of the elastic constants causes sound scattering and attenuation. In the limit of the wavelength being much larger than the characteristic spatial scale of the inhomogeneity this mechanism is equivalent to Rayleigh scattering and results in k^4 scaling. If the elastic constant variations have slowly decaying, power-law-like correlations, the theory predicts a logarithmic correction to Rayleigh scattering [9, 15]. Other physical approaches, *e.g.* local oscillator [11, 13, 14] and random matrix [16–18] models, can also be used to derive the Rayleigh scattering

law. For this reason, Rayleigh scaling cannot serve to distinguish between different models [11].

Three recent studies came to different conclusions regarding the applicability of the fluctuating elasticity theory. First, Caroli and Lemaître [19] analyzed a version of the theory derived from microscopic equations of motion. They obtained all the parameters needed to calculate sound attenuation from the theory from the same simulations that were used to test the theoretical predictions. They showed that this version of the theory underestimates sound attenuation by about two orders of magnitude.

Second, Kapteijns *et al.* [20] analyzed the dependence of the sound attenuation on a parameter δ , which “resembles” changing the stability of the amorphous solid. They calculated the disorder parameter [10] of the fluctuating elasticity theory, sidestepping the issue of the definition of local elastic constants by replacing fluctuations of local elastic constants by the sample-to-sample fluctuations. Kapteijns *et al.* showed that the disorder parameter and the sound damping coefficient have the same dependence on δ .

Finally, Mahajan and Pica Ciamarra [21] argued that sound attenuation is proportional to the square of the disorder parameter according to a version of fluctuating elasticity theory that incorporates an elastic correlation length [11, 22]. They relied upon a relation between the boson peak, the speed of sound, and an elastic correlation length to show that the speed of sound and the boson peak frequency can be used to infer the change of the sound damping coefficient. In contrast to Caroli and Lemaître, neither Kapteijns *et al.* nor Mahajan and Pica Ciamarra calculated the values of the sound damping coefficient, but rather the variation of the sound attenuation for different glasses.

Here we analyze sound attenuation using the microscopic equations of motion. Our goal is to understand the microscopic origin of the low temperature sound attenuation, rather than derive or validate a model. We derive an exact equation of motion for an auto-correlation function that can be used to determine sound attenua-

tion. We identify the self-energy and show that its real part reproduces the non-Born contribution to the zero-temperature wave propagation coefficients of amorphous solids. The imaginary part of the self-energy is the origin of sound attenuation. We show that sound attenuation calculated this way agrees with that obtained from independent simulations. The small wavevector expansion shows that the limiting k^4 sound attenuation originates from the same physics as the non-Born contribution to the elastic constants, *i.e.* from the non-affine displacements. More precisely, attenuation of the sound wave is primarily determined by the contribution to the non-Born part of the wave propagation coefficient from a shell of frequencies around the frequency of the sound wave.

Sound attenuation: microscopic analysis.— We start from microscopic equations of motion for small displacements of N spherically symmetric particles of unit mass comprising our model 3D amorphous solid,

$$\partial_t^2 \mathbf{u}_i = - \sum_j \mathcal{H}_{ij} \cdot \mathbf{u}_j. \quad (1)$$

Here \mathbf{u}_i is the displacement of the i th particle from its inherent structure (potential energy minimum) position \mathbf{R}_i and \mathcal{H} is the Hessian calculated at the inherent structure,

$$\mathcal{H}_{ij} = - \frac{\partial \mathbf{F}_i(\{\mathbf{R}_m\})}{\partial \mathbf{R}_j}, \quad (2)$$

with \mathbf{F}_i being the total force acting on particle i [23].

To derive an expression for the sound attenuation parameter we use a slightly modified procedure proposed by Gelin *et al.* [9]. We assume that at $t = 0$ the particles are displaced from their equilibrium positions according to $\mathbf{u}_i(t = 0) = \hat{\mathbf{e}} \exp(-i\mathbf{k} \cdot \mathbf{R}_i)$, $\dot{\mathbf{u}}_i(t = 0) = 0$, where $\hat{\mathbf{e}}$ is a unit vector and wavevector \mathbf{k} is one of the wavevectors allowed by periodic boundary conditions. We focus on the auto-correlation function of the single-particle displacement averaged over the whole system, $C(t) = N^{-1} \sum_i \mathbf{u}_i^*(t = 0) \cdot \mathbf{u}_i(t)$. We anticipate that in the limit of small wavevectors \mathbf{k} the auto-correlation function will exhibit damped oscillations, $C(t) \propto \cos(vkt) \exp(-\Gamma(k)t/2)$, and we will identify v as the speed of sound and $\Gamma(k)$ as the damping coefficient.

We note that solving Eqs. (1) with our initial conditions is equivalent to solving

$$\partial_t^2 \mathbf{a}_i = - \sum_j \mathcal{H}_{ij}(\mathbf{k}) \cdot \mathbf{a}_j, \quad (3)$$

where $\mathcal{H}(\mathbf{k})$ is the wavevector-dependent Hessian, $\mathcal{H}_{il}(\mathbf{k}) = \mathcal{H}_{il} \exp[i\mathbf{k} \cdot (\mathbf{R}_i - \mathbf{R}_l)]$, with initial conditions $\mathbf{a}_i(t = 0) = \hat{\mathbf{e}}$, $\dot{\mathbf{a}}_i(t = 0) = 0$. In terms of the new variables, $C(t) = N^{-1} \sum_i \mathbf{a}_i(t = 0) \cdot \mathbf{a}_i(t)$.

To analyze $C(t)$ we use the standard projection operator approach [24]. We define a scalar product of two displacement vectors, \mathbf{a}_i and \mathbf{b}_j , $i, j = 1, \dots, N$,

$\langle a|b \rangle = \sum_i \mathbf{a}_i^* \cdot \mathbf{b}_i$. Next, we define a unit vector $|1\rangle$ with components $\mathbf{1}_i = N^{-1/2} \hat{\mathbf{e}}$, and projection operator \mathcal{P} on the unit vector, $\mathcal{P} = |1\rangle \langle 1|$ and orthogonal projection \mathcal{Q} , $\mathcal{Q} = \mathcal{I} - |1\rangle \langle 1|$ where \mathcal{I} is the identity matrix.

Using the projection operator approach we obtain the following expression for the Fourier transform $C(\omega) = \int_0^\infty C(t) \exp(i(\omega + i\epsilon)t) dt$ of the displacement auto-correlation function,

$$C(\omega) = \frac{i(\omega + i\epsilon)}{(\omega + i\epsilon)^2 - \langle 1|\mathcal{H}(\mathbf{k})|1 \rangle + \Sigma(\mathbf{k}; \omega)}, \quad (4)$$

where the self-energy $\Sigma(\mathbf{k}; \omega)$ reads

$$\Sigma(\mathbf{k}; \omega) = \left\langle 1 \left| \mathcal{H}(\mathbf{k}) \mathcal{Q} \frac{1}{-(\omega + i\epsilon)^2 + \mathcal{Q}\mathcal{H}(\mathbf{k})\mathcal{Q}} \mathcal{Q}\mathcal{H}(\mathbf{k}) \right| 1 \right\rangle. \quad (5)$$

Equations (4-5) are exact. While it is straightforward to calculate $\langle 1|\mathcal{H}(\mathbf{k})|1 \rangle$, evaluation of the self-energy requires inversion of a large-dimensional matrix for each allowed wavevector. To make the numerical effort manageable, in the denominator in Eq. (5) we approximate $\mathcal{H}(\mathbf{k})$ by \mathcal{H} . This approximation does not influence the small wavevector properties.

In the small wavevector limit, the first non-trivial term in the denominator in Eq. (4), $\langle 1|\mathcal{H}(\mathbf{k})|1 \rangle$, can be expressed in terms of the Born contributions to the zero-temperature wave-propagation coefficients [25],

$$\langle 1|\mathcal{H}(\mathbf{k})|1 \rangle = \rho^{-1} \hat{\mathbf{e}}_\alpha A_{\alpha\beta\gamma\delta}^{\text{Born}} k_\beta \hat{\mathbf{e}}_\gamma k_\delta \quad (6)$$

where $\rho = N/V$ is the number density, Greek indices denote Cartesian components, the Einstein summation convention for Greek indices is hereafter adopted, and $A_{\alpha\beta\gamma\delta}^{\text{Born}} = N^{-1} \sum_j A_{j\alpha\beta\gamma\delta}^{\text{Born}}$, where

$$A_{j\alpha\beta\gamma\delta}^{\text{Born}} = \frac{\rho}{2} \sum_{l \neq j} \frac{\partial^2 V(R_{jl})}{\partial R_{j\alpha} \partial R_{j\gamma}} R_{jl\beta} R_{jl\delta} \quad (7)$$

is the local wave-propagation coefficient. In the absence of the self-energy term, Eq. (4) predicts the Born value of the speed of sound and no damping. Both the renormalization of the sound speed and the sound attenuation originate from the self-energy.

The self-energy can be calculated using the eigenvalues and eigenvectors of the Hessian. In the thermodynamic limit, when the spectrum of the Hessian becomes continuous, we can use the Plemelj identity to identify the imaginary component of the self-energy [26], which is responsible for sound attenuation. The real $\Sigma'(\mathbf{k}; \omega)$ and imaginary $\Sigma''(\mathbf{k}; \omega)$ parts of the self-energy read,

$$\Sigma'(\mathbf{k}; \omega) = \mathcal{P} \int d\Omega \Upsilon(\mathbf{k}, \Omega) (\Omega^2 - \omega^2)^{-1}, \quad (8)$$

$$\Sigma''(\mathbf{k}; \omega) = \frac{\pi}{2\omega} \Upsilon(\mathbf{k}, |\omega|), \quad (9)$$

where \mathcal{P} denotes the Cauchy principal value. The function $\Upsilon(\mathbf{k}, \Omega)$ is defined through the sum over eigenvectors

\mathcal{E}_p of the Hessian matrix with non-zero [27] eigenvalues Ω_p^2 such that $\Omega_p \in [\Omega, \Omega + d\Omega]$,

$$\Upsilon(\mathbf{k}, \Omega) = (1/d\Omega) \sum_{\Omega_p \in [\Omega, \Omega + d\Omega]} |\langle 1 | \mathcal{H}(\mathbf{k}) \mathcal{Q} | \mathcal{E}_p \rangle|^2. \quad (10)$$

To evaluate the displacement auto-correlation function we need to find complex poles of the denominator at the right-hand-side of Eq. (4). In the small wavevector limit this can be done perturbatively,

$$\omega_{\pm} = \pm vk - i\Sigma''(\mathbf{k}; vk)/(2vk) \quad (11)$$

where the renormalized speed of sound v is given by

$$v^2 = \lim_{k \rightarrow 0} k^{-2} [\langle 1 | \mathcal{H}(\mathbf{k}) | 1 \rangle - \Sigma'(\mathbf{k}; 0)]. \quad (12)$$

The last term in Eq. (11) is our main result, sound damping in zero-temperature amorphous solids is determined by $\Upsilon(\mathbf{k}, \Omega)/\Omega^2$ calculated at the wave's frequency, $\Omega = vk$,

$$\Gamma(k) = \frac{\Sigma''(\mathbf{k}; vk)}{vk} = \frac{\pi}{2} \frac{\Upsilon(\mathbf{k}, vk)}{(vk)^2}. \quad (13)$$

Note that $\Upsilon(\mathbf{k}, \Omega)/\Omega^2$ is the same function that, after integration over the whole frequency spectrum, determines the renormalization of the wave propagation coefficients. Also, v , $\Gamma(k)$, and related quantities defined below depend on the angle between the polarization of the initial condition $\hat{\mathbf{e}}$ and the direction of the wavevector $\hat{\mathbf{k}}$.

To verify Eqs. (12-13) we calculated v and $\Gamma(k)$ for zero-temperature glasses analyzed in Ref. [7]. These glasses were obtained by instantaneously quenching supercooled liquids equilibrated using the swap Monte Carlo algorithm [28] at different parent temperatures T_p to their inherent structures using the fast inertial relaxation engine minimization [29]. The glasses consist of spherically symmetric, polydisperse particles which interact via a potential $\propto r^{-12}$, with a smooth cutoff, see Refs. [7, 28] for details. The parent temperature controls the glass's stability and thus its properties [7, 30, 31].

We calculated eigenvalues and eigenvectors of the Hessian using ARPACK [32] and Intel Math Kernel Library [33], and evaluated v and $\Gamma(k)$ for the longitudinal, $\hat{\mathbf{e}} \parallel \hat{\mathbf{k}}$, and the transverse, $\hat{\mathbf{e}} \perp \hat{\mathbf{k}}$, sound. Fig. 1 shows results for three parent temperatures: $T_p = 0.2$, which is approximately equal to the onset temperature; $T_p = 0.085$, which is between the mode-coupling temperature $T_c \approx .108$ and the estimated glass transition temperature $T_g \approx 0.072$; and $T_p = 0.062$, which gives an ultrastable glass.

For all three parent temperatures there is excellent agreement between results of Eqs. (12,13) and independently estimated [7] transverse and longitudinal sound speeds, and transverse and longitudinal sound damping coefficients. At small wavevectors we recover Rayleigh scaling, $\Gamma \propto k^4$, but the theory also accurately predicts

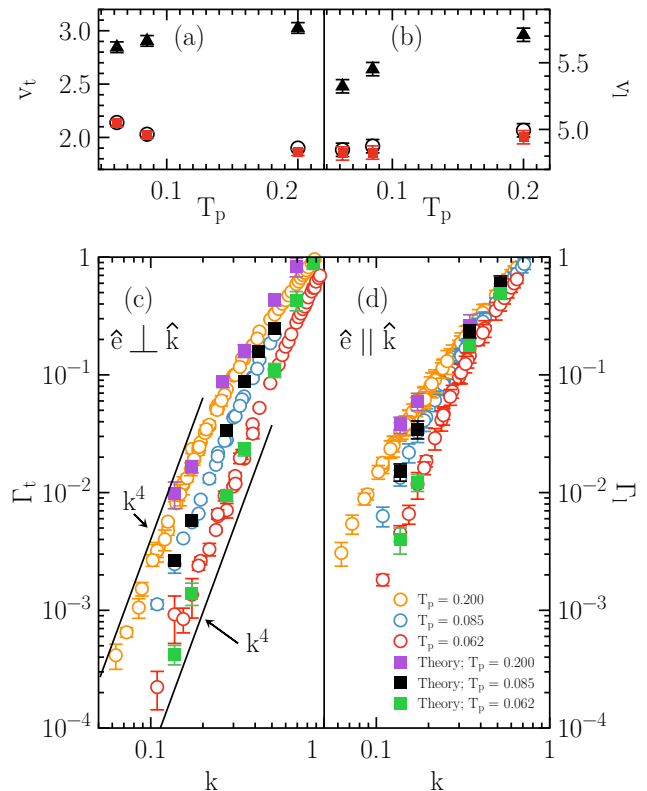


FIG. 1. Upper panels: the transverse (a) and longitudinal (b) speed of sound obtained from the theory, Eq. (12), (red squares) and calculated from the elastic constants (black circles) as a function of parent temperature T_p . The black triangles are the Born values of the speed of sound. Lower panels: the transverse (a) and longitudinal (b) damping coefficients obtained from the theory, Eq. (13), (squares) and obtained from sound simulations [7] (circles) for different parent temperatures. Rayleigh scaling $\Gamma \propto k^4$ is recovered at small wavevectors.

sound damping for wavevectors outside the Rayleigh scaling regime. The predicted damping coefficients depart from the simulation results for larger wavevectors, but at larger wavevectors the assumptions used to find the poles, Eq. (11), become invalid. We also show in Fig. 1(a-b) the Born contributions to sound speeds, and find that the renormalization of the speed of sound decreases with decreasing T_p .

Non-affine displacements vs. elasticity fluctuations.— To get some physical insight into the origin of sound attenuation in zero-temperature amorphous solids we examine the small wavevector expansion of $\langle 1 | \mathcal{H}(\mathbf{k}) \mathcal{Q} | \mathcal{E}_p \rangle$,

$$\begin{aligned} \langle 1 | \mathcal{H}(\mathbf{k}) \mathcal{Q} | \mathcal{E}_p \rangle &= -iN^{-1/2} \sum_j \Xi_{j\beta\gamma} \hat{e}_\beta k_\gamma \cdot \mathcal{E}_{pj} \quad (14) \\ &+ \rho^{-1} N^{-1/2} \sum_j [A_{j\alpha\beta\gamma\delta}^{\text{Born}} - \hat{e}_\alpha \hat{e}_\mu A_{\mu\beta\gamma\delta}^{\text{Born}}] \hat{e}_\gamma k_\beta k_\delta \mathcal{E}_{pj\alpha} + o(k^2). \end{aligned}$$

In Eq. (14) \mathcal{E}_{pj} denotes the part of the p th eigenvec-

tor of the Hessian corresponding to particle j and $\mathcal{E}_{pj\alpha}$ denotes its Cartesian components. Furthermore, $\Xi_{j\beta\gamma}$ denotes the vector field describing forces resulting from affine deformations of the particles,

$$\Xi_{j\beta\gamma} = - \sum_{l \neq j} \frac{\partial^2 V(R_{jl})}{\partial R_{j\beta} \partial R_{jl}} R_{jl\gamma}. \quad (15)$$

Finally, the last term in Eq. (14) accounts for the spatial variation of the local Born wave propagation coefficients.

As discussed in the literature [34–36], vector field $\Xi_{j\beta\gamma}$ describes the influence of an amorphous solid's non-affine displacements on the solid's properties. In particular, it follows from the combination of Eqs. (8), (12) and (14) that the renormalization of the wave propagation coefficients originates from the first term in Eq. (14),

$$\lim_{k \rightarrow 0} k^{-2} \Sigma'(\mathbf{k}; 0) = N^{-1} \int d\Omega \Theta(\Omega) \Omega^{-2} \quad (16)$$

where $\Theta(\Omega)$ is defined analogously to $\Upsilon(\mathbf{k}, \Omega)$,

$$\Theta(\Omega) = (1/d\Omega) \sum_{\Omega_p \in [\Omega, \Omega+d\Omega]} \left| \Xi_{p\beta\gamma} \hat{e}_\beta \hat{k}_\gamma \right|^2 \quad (17)$$

with $\Xi_{p\beta\gamma} = N^{-1/2} \sum_j \Xi_{j\beta\gamma} \cdot \mathcal{E}_{pj}$. Equations (16-17) reproduce the exact expression for the non-Born contribution to the wave propagation coefficients derived from the analysis of the non-affine displacements [34, 35, 37].

While only the first term in Eq. (14) determines the renormalization of the wave propagation coefficients, both terms contribute to sound attenuation,

$$\Gamma(k) = \frac{\pi}{2v^2} [\Theta(vk) + k^2 \Delta(vk)] \quad (18)$$

where $\Delta(\Omega)$ is defined analogously to $\Upsilon(\mathbf{k}, \Omega)$,

$$\Delta(\Omega) = (1/d\Omega) \sum_{\Omega_p \in [\Omega, \Omega+d\Omega]} \left| \delta A_{p\beta\gamma\delta} \hat{k}_\beta \hat{e}_\gamma \hat{k}_\delta \right|^2 \quad (19)$$

with $\delta A_{p\beta\gamma\delta} = \rho^{-1} N^{-1/2} \sum_j \left[A_{j\alpha\beta\gamma\delta}^{\text{Born}} - \hat{e}_\alpha \hat{e}_\mu A_{\mu\beta\gamma\delta}^{\text{Born}} \right] \mathcal{E}_{pj\alpha}$.

The physical content of the second term in Eq. (18) resembles that of the fluctuating elasticity theory. However, this interpretation is likely somewhat naive and, moreover, it is the first term that makes the dominant contribution to the damping coefficient, see Fig. 2.

Discussion.— According to our microscopic analysis, sound attenuation in zero-temperature amorphous solids is primarily determined by internal forces induced by initial affine displacements of the particles, *i.e.* by the physics of non-affine displacement fields. Quantitatively, the damping coefficient is proportional to the non-affine contribution to the wave propagation coefficients from the frequency equal to the frequency of the sound wave.

It is not trivial that our analysis reproduces the Rayleigh scaling of sound damping coefficients. This fact results from the frequency dependence of Θ and Δ , which deserves further theoretical study [38].

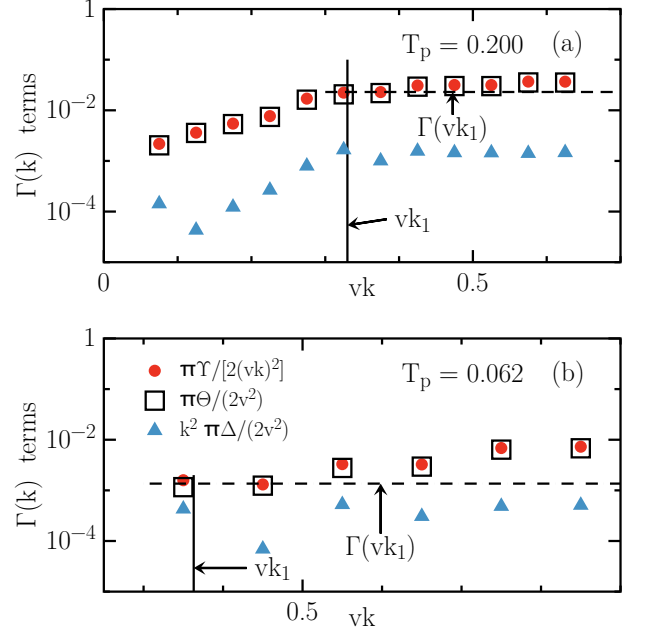


FIG. 2. The terms that contribute to the transverse sound attenuation for $k_1 = 0.13722$ given by Eq. 18 for $T_p = 0.200$ (a) and $T_p = 0.062$ (b). The vertical lines marks the frequency $vk_1 = v_t k_1$, where v_t is the transverse speed of sound, and the horizontal line is the sound attenuation calculated in simulations from Ref. [7]. The value of $\pi\Upsilon(\mathbf{k}_1, vk_1)/[2(vk_1)^2]$ gives the damping for k_1 .

The mechanism of the attenuation revealed by our microscopic analysis was mentioned by Caroli and Lemaître in Ref. [19]. It was investigated in Ref. [39], where Caroli and Lemaître considered separately the effects of the long-wavelength, elastic continuum-like, and small-scale, primarily non-affine, motions with the small-scale motions being the scatterers for the long-wavelength ones. Reference [39] analyzed sound propagation and attenuation in two-dimensional amorphous solids, which are somewhat special in that almost all of their low frequency modes are extended [40, 41]. In 3D amorphous solids there is a clear distinction between low-frequency quasi-localized and extended modes [30, 40]. We attempted to quantify the relative contributions of the extended and quasi-localized modes to the sound attenuation as given by Eq. (13) or (18), and we did not find convincing evidence for the dominance of either one. This fact is a bit surprising in view of the clear correlation between the amplitude of the quasi-localized modes' density and the sound attenuation coefficient [7] and deserves further investigation.

Damart *et al.* [36] demonstrated that the non-affine displacement field was responsible for high-frequency harmonic dissipation in a simulated amorphous SiO_2 . Therefore, it appears that non-affine displacements are responsible for dissipation over the full frequency range,

but further theoretical development is needed to connect the low-frequency and high-frequency theories.

We emphasize that the spatially varying elastic constants postulated by the fluctuating elasticity theory are usually interpreted as locally defined renormalized elastic constants rather than their Born contributions. This interpretation allowed Kapteijns *et al.* to substitute sample-to-sample fluctuations of elastic constants for the fluctuations of the local elastic constants. Thus, in spite of the resemblance between the second term in Eq. (18) and the formula derived from fluctuating elasticity theory, these expressions are not equivalent.

Finally, we note that calculating sound attenuation using Eq. (13) or (18) is somewhat numerically demanding but more straightforward than analyzing the time dependence of the velocity or displacement auto-correlation functions.

We thank A. Ninarello for generously providing equilibrated configurations at very low parent temperatures and E. Bouchbinder for comments on the manuscript. We gratefully acknowledge the support of NSF Grant No. CHE 1800282.

-
- [1] L. D. Landau and E. M. Lifshitz, *Theory of Elasticity* (Pergamon, New York, 1975).
- [2] P. C. Martin, O. Parodi and P. S. Pershan, “Unified Hydrodynamic Theory for Crystals, Liquid Crystals, and Normal Fluids”, *Phys. Rev. A* **6**, 2401 (1972).
- [3] See, *e.g.*, C. Masciovecchio, G. Baldi, S. Caponi, L. Comez, S. Di Fonzo, D. Fioretto, A. Fontana, A. Gessini, S.C. Santucci, F. Sette, G. Vilianni, P. Vilmercati and G. Ruocco, “Evidence for a Crossover in the Frequency Dependence of the Acoustic Attenuation in Vitreous Silica”, *Phys. Rev. Lett.* **97**, 035501 (2006).
- [4] R.C. Zeller and R.O. Pohl, “Thermal conductivity and specific heat of noncrystalline solids”, *Phys. Rev. B* **4**, 2029 (1971).
- [5] M. P. Zaitlin and A. C. Anderson, “Phonon thermal transport in noncrystalline materials”, *Phys. Rev. B* **12**, 4475 (1975).
- [6] H. Mizuno and A. Ikeda, “Phonon transport and vibrational excitations in amorphous solids”, *Phys. Rev. E* **98**, 062612 (2018).
- [7] L. Wang, L. Berthier, E. Flenner, P. Guan and G. Szamel, “Sound attenuation in stable glasses”, *Soft Matter* **15**, 7018 (2019).
- [8] A. Moriel, G. Kapteijns, C. Rainone, J. Zylberg, E. Lerner and E. Bouchbinder, “Wave attenuation in glasses: Rayleigh and generalized-Rayleigh scattering scaling”, *J. Chem. Phys.* **151**, 104503 (2019).
- [9] S. Gelin, H. Tanaka and A. Lemaître, “Anomalous phonon scattering and elastic correlations in amorphous solids”, *Nature Materials* **15**, 1177 (2016).
- [10] W. Schirmacher, “Thermal conductivity of glassy materials and the ‘boson peak’” *Europhys. Lett.*, 2006, **73**, 892.
- [11] W. Schirmacher, “Some comments on fluctuating-elasticity and local oscillator models for anomalous vibrational excitations in glasses”, *J. Non-Cryst. Solids* **357**, 518 (2011).
- [12] E.A.A. Pogna, A.I. Chumakov, C. Ferrante, M.A. Ramos and T. Scopigno, “Tracking the Connection between Disorder and Energy Landscape in Glasses Using Geologically Hyperaged Amber”, *J. Phys. Chem. Lett.*, **10** 427 (2019).
- [13] U. Buchenau, Yu. M. Galperin, V.L. Gurevich, D.A. Parshin, M.A. Ramos and H.R. Schober, “Interaction of soft modes and sound waves in glasses”, *Phys. Rev. B*, **46**, 2798 (1992).
- [14] V.L. Gurevich, D.A. Parshin, J. Pelous and H.R. Schober, “Theory of low-energy Raman scattering in glasses”, *Phys. Rev. B*, **48**, 16318 (1993).
- [15] B. Cui and A. Zaccone, “Analytical prediction of logarithmic Rayleigh scattering in amorphous solids from tensorial heterogeneous elasticity with power-law disorder”, *Soft Matter* **16**, 7797 (2020).
- [16] T.S. Grigera, V. Martin-Mayor, G. Parisi, P. Urbani and P. Verrocchio, “On the high-density expansion for Euclidean random matrices”, *J. Stat. Mech.* **2011** P02015 (2011).
- [17] D.A. Conyuh and Y.M. Beltukov, “Universal Vibrational Properties of Disordered Systems in Terms of the Theory of Random Correlated Matrices”, *JETP Letters* **112**, 513 (2020).
- [18] C. Ganter and W. Schirmacher, “Rayleigh scattering, long-time tails, and the harmonic spectrum of topologically disordered systems”, *Phys. Rev. B*, **82**, 094205 (2010).
- [19] C. Caroli and A. Lemaître, “Fluctuating Elasticity Fails to Capture Anomalous Sound Scattering in Amorphous Solids”, *Phys. Rev. Lett.* **123**, 055501 (2019).
- [20] G. Kapteijns, D. Richard, E. Bouchbinder, and E. Lerner, “Elastic moduli fluctuations predict wave attenuation rates in glasses”, *J. Chem. Phys.* **154**, 081101 (2021).
- [21] S. Mahajan and M. Pica Ciamarra, “Unifying description of the vibrational anomalies of amorphous materials”, arXiv:2106.04868.
- [22] W. Schirmacher, C. Tomaras, B. Schmid, G. Baldi, G. Vilianni, G. Ruocco, and T. Scopigno, “Sound attenuation and anharmonic damping in solids with correlated disorder”, *Condensed Matter Physics* **13**, 23606 (2010).
- [23] Note that each element \mathcal{H}_{ij} is a 3x3 tensor.
- [24] R. Zwanzig, *Nonequilibrium Statistical Mechanics*, (Oxford, New York, 2002).
- [25] D. C. Wallace, *Thermodynamics of Crystals* (Wiley, New York, 1972).
- [26] For a discussion of the importance of the thermodynamic limit see R.D. Mattuck, *A Guide to Feynman Diagrams in the Many-Body Problem* (Dover, New York, 1992), Appendix H.
- [27] In d spatial dimensions the Hessian matrix has a d -degenerate zero eigenvalue corresponding to d independent unit vectors; these eigenvalues are removed by the orthogonal projection in Eq. (5).
- [28] A. Ninarello, L. Berthier, and D. Coslovich “Models and algorithms for the next generation of glass transition studies”, *Phys. Rev. X* **7**, 021039 (2017).
- [29] E. Bitzek, P. Koskinen, F. Gähler, M. Moseler and P. Gumbsch, “Structural Relaxation Made Simple”, *Phys. Rev. Lett.* **97**, 170201 (2006).
- [30] L. Wang, A. Ninarello, P. Guan, L. Berthier, G. Szamel

- and E. Flenner, *Nat. Commun.* **10**, 26 (2019).
- [31] M. Ozawa, L. Berthier, G. Biroli, A. Rosso and G. Tarjus, *Proc. Natl Acad. Sci. USA* **115**, 6656 (2018).
- [32] <http://www.caam.rice.edu/software/ARPACK/>.
- [33] <https://software.intel.com/en-us/mkl/>.
- [34] C. Maloney and A. Lemaître “Universal Breakdown of Elasticity at the Onset of Material Failure”, *Phys. Rev. Lett.* **93**, 195501 (2004).
- [35] A. Lemaître and C. Maloney, “Sum Rules for the Quasi-Static and Visco-Elastic Response of Disordered Solids at Zero Temperature”, *J. Stat. Phys.* **123**, 415 (2006).
- [36] T. Damart, A. Tanguy and D. Rodney, “Theory of harmonic dissipation in disordered solids”, *Phys. Rev. B* **95**, 054203 (2017).
- [37] Function $\Theta(\Omega)$ is closely related to function $\Gamma_{\alpha\beta\kappa\chi}(\omega)$ introduced and evaluated by Lemaître and Maloney, see Eq. (32) of Ref. [35].
- [38] Rayleigh scaling can be recovered analytically within an approximate perturbative calculation in which the eigenvectors of the Hessian are approximated by plane waves.
- [39] C. Caroli and A. Lemaître, “Key role of retardation and non-locality in sound propagation in amorphous solids as evidenced by a projection formalism”, *J. Chem. Phys.* **153**, 144502 (2020).
- [40] H. Mizuno, H. Shiba, and A. Ikeda, “Continuum limit of the vibrational properties of amorphous solids”, *Proc. Natl. Acad. Sci. U.S.A.* **114**, E9767 (2017).
- [41] L. Wang, G. Szamel and E. Flenner, “Low-frequency excess vibrational modes in two-dimensional glasses”, arXiv:2107.01505.